Multi-Objective Transmission Expansion Planning for Flexible Grid Infrastructure Toward a Low-Carbon Energy Era

Luiz Eduardo de Oliveira
Dept. of Elect. and Compt. Engineering, FEUP
Porto, Portugal
luiz.eduardo@fe.up.pt

Phillipe Vilaça Gomes
Baringa
Madrid, Spain
phillipe.vilacagomes@baringa.com

João Tomé Saraiva
Dept. of Elect. and Compt. Engineering, FEUP
Porto, Portugal
jsaraiva@fe.up.pt

***Abstract*—The global shift toward a low-carbon era requires a greater integration of Renewable Energy Sources (RESs) and the phase-out of power plants fueled by non-Renewable Energy Sources (nRESs). Meanwhile, Climate Change (CC) and Extreme Weather Events (EWEs) are increasingly affecting energy systems, introducing new layers of uncertainties in long- and short-term power system planning. This study presents a Multi-Objective Transmission Expansion Planning (MO-TEP) model aimed at improving the flexibility of the ERCOT grid while reducing Greenhouse Gas (GHG) emissions. This model uses real data from Form EIA-860 for RESs penetration and decommissioning of nRESs. The ACTIVSg2000 test case, a synthetic ERCOT-like system, validates the study. The findings emphasize the importance of incorporating high-impact, low-probability (HILP) events into TEP decisions and highlight the critical role of grid flexibility in enhancing resilience. This research contributes to a more reliable and sustainable electricity network capable of adapting to evolving environmental and operational conditions.**

***Index Terms*—Climate Change, Flexibility, Low-Carbon Energy Transition, Multi-Objective Optimization, NSGA-II, Transmission Expansion Planning.**

I. Introduction

A global movement towards a low-carbon revolution is gaining momentum in a world marked by the repercussions of High-Impact, Low-Probability (HILP) events, namely Climate Change (CC) and Extreme Weather Events (EWEs) [1]. For instance, in 2021, Texas was hit by a snowstorm, causing extensive damage [2]–[6]. The energy transition is a fundamental shift for modern power systems. The Paris Agreement outlines three pathways to accelerate this transition: *a)* increasing electricity generation from renewable energy sources (RESs); *b)* decommissioning non-renewable sources (nRESs), particularly nuclear and coal-fired power plants; and *c)* electrifying the transportation sector [7], [8]. These changes are essential to achieving net-zero carbon emissions by 2050 and mitigating the adverse effects of CC and EWEs [9].

Recognizing the link between ecological balance and sustainable development, nations are redefining energy policies to build a greener electricity matrix [9], [10]. This trend pushes decision-makers to assess rising RESs penetration and its impacts, adding new layers of uncertainties in long- and short-term planning, respectively: CC and EWEs [11]–[14].

Since TEP is a capital-intensive process, it requires a clear and well-justified decision-making framework [15]. Large-scale investments in transmission infrastructure must account for future electricity consumption patterns and the evolving generation mix. This study presents a multi-objective TEP model that aims to enhance the flexibility of the Electric Reliability Council of Texas (ERCOT) grid while reducing Greenhouse Gas (GHG) emissions, and meanwhile considering the survey Form EIA-860 as a guideline for generator-level specific information about commissioning planned generators and decommissioning coal-fired power plants in the U.S. [16].

To validate the proposed approach, the ACTIVSg2000 test case [17], a synthetic power system modeled after ERCOT's grid, is used. The analysis highlights:

- The critical role of incorporating HILPs, such as CC and EWEs, into TEP decision-making.
- The correlation between grid flexibility and the power system's ability to adapt to extreme conditions.

By integrating these considerations, this study contributes to a resilient and sustainable electricity network, ensuring long-term reliability and efficiency amid evolving challenges.

II. Multi-Objective Transmission Expansion Planning

TEP strategically guides power system development to ensure economic and technical reliability. By upgrading infrastructure, creating new corridors, or adding reinforcements to transmission networks, TEP determines when, where, and how to expand transmission. By incorporating secondary goals, the TEP becomes a Multi-Objective (MO-TEP), capable of increasing the energy transport range, improving reliability and flexibility, which can reduce GHG emissions [18].

A. Mathematical Formulation

TEP is an NP-hard problem integrating integer and continuous decision variables in an optimization framework. As a Mixed Integer Non-Linear Programming (MINLP) problem,

979-8-3315-1278-1/25/$31.00

the TEP task requires substantial computational effort. In this paper, the comprehensive Multi-Objective Function (MOF) described in Eq. (1) is composed by three objectives:

- **minimize total costs** (Z_1), which includes costs incurred over the planning horizon, such as investment in new transmission assets ($C^{inv}_{t,\sigma}$), unreliability costs ($C^{unr}_{t,\sigma}$), and Operation and Maintenance (o&m) expenditures ($C^{o\&m}_{t,\sigma}$).
- **minimize GHG emissions** (Z_2), by accounting for Carbon Dioxide (CO_2), Nitrous Oxide (N_2O), and Fluorinated gases such Sulfur Hexafluoride (SF_6);
- **maximize flexibility** (Z_3), by assessing the Relative Flexibility Index (RFI).

$$MOF = (Z_1, Z_2, Z_3) \tag{1}$$

B. Expansion Planning Task Formulation

The initial stage focuses on solving the multi-stage deterministic TEP problem, where a solution is considered feasible if the investment portfolio guarantees proper system operation with $EENS = 0$. Expansion decisions must be made in the present timeframe when failures and operative and maintenance costs are only forecasted. This temporal imposition necessitates solving the mathematical formulation outlined from Equations (2) to (28) to ensure network resilience stressed operative conditions and mitigate associated impacts.

$$\min_{\substack{x\in X\\ g,\tau,\varphi\\ \mathcal{L}}} Z_1 = \rho \sum_{\sigma\in\Omega_6}\sum_{t\in\Omega_1}\left[C^{inv}_{t,\sigma} + C^{o\&m}_{t,\sigma} + C^{unr}_{t,\sigma}\right] \tag{2}$$

In this model, Ω_1 denotes the set of stages; the initial transmission topology (x_0) and all new projects (x) are encompassed by Ω_2. Meanwhile, Ω_3 represents all buses within the network. Additionally, Ω_4 signifies the set of all non-renewable generators, while Ω_5 contains all renewable sources. Ω_6 is the set of all economic and operative N-1 scenarios.

*1) **Investment costs**:* As observed in [12]–[14], the TEP problem is structured as a MINLP with upper and lower levels. The upper-level problem, delineated by Equations (3) and (4), determines the values of $C^{inv}_{t,\sigma}$, while the lower level provide $C^{o\&m}_{t,\sigma}$ and $C^{unr}_{t,\sigma}$. Therefore, the manager-worker relationship between both levels is noteworthy. In the upper level, the integer decision variables (x) symbolize the planned investments for new transmission assets, encompassing overhead lines, cables, and transformers.

$$\min_{\{x\in X\}} C^{inv}_{t,\sigma} = \sum_{(i,j)\in\Omega_2} \frac{x_{(i,j),t}\cdot K_{(i,j)}}{(1+R+\varepsilon_\sigma)^t} \tag{3}$$

subject to:

$$0 \le \sum_{(i,j)\in\Omega_2} x_{(i,j),t} \le \overline{x}_{(i,j)} \tag{4}$$

In Eq. (3), R denotes the annual interest rate, while ε expresses its long-term economic uncertainty over the years; K expresses the projected initial cost for each project.; and t signifies each stage within the planning horizon.

*2) **Operation and Maintenance costs**:* The lower-level subproblem assesses the costs associated with continuous decision variables, including generation (g), curtailment of primary sources (τ), overload (φ), as well as artificial variables representing planned outages (ϖ) and failures (f). These variables are determined using an Interior Point Solver [19], applied to the problem outlined from Equations (5) and (22), for all $t \in \Omega_1 \wedge \sigma \in \Omega_6$, and subject to the constraints detailed from Equations (6) to (21), (23) and (24).

Operation costs in Eq. (5) include: $\mathcal{G}$, as the function representing the nominal cost per MWh for each generator; and η, the curtailment penalty of 3 USD per wasted renewable kWh [20]. The overload penalty ϕ is fixed at 1 USD/kWh.

$$\begin{aligned}\min_{\substack{x\in X\\ g,\tau,\varphi}} C^{o\&m}_{t,\sigma} = \phi \sum_{(i,j)\in\Omega_2} \varphi_{(i,j),t,\sigma}\cdot(x+x_0) + \\ \eta\sum_{r\in\Omega_5}\tau_{r,t,\sigma} + \sum_{i\in\Omega_3} g_{i,t,\sigma}\cdot\mathcal{G}_{i,t}\end{aligned} \tag{5}$$

The rise in RESs adoption, particularly from photovoltaic arrays and wind turbines, brings about short-term variations in energy production and demand patterns. Due to the unpredictable nature of these sources and demand, it is crucial to strengthen power infrastructures addressing fluctuating load and generation patterns.

As described in Eq. (6), the total generation (g) at each bus is determined by summing the contributions from non-renewable sources (N) and renewable sources, specifically hydro (H), wind (W), and solar (Φ), while subtracting the curtailed portion of primary sources (τ). Additionally, Equation (6) accounts for: short-term wind fluctuation (w) modeled as a Weibull Probability Density Function (PDF); photovoltaic variations (s) addressed by a Beta PDF; (h) hydro inflow uncertainties and short-term demand fluctuations (d) depicted by Gaussian PDFs [13], [21], [22].

$$\begin{aligned}g_{i,t,\sigma} = \sum_{n\in\Omega_4} N_{i,n,t} \;+ \\ \sum_{r\in\Omega_5}\left[\Phi_{i,r,t} + W_{i,r,t} + H_{i,r,t} - \tau_{i,r,t}\right] \;+ \\ \sum_{r\in\Omega_5}\left[s_{i,r,t,\sigma} + w_{i,r,t,\sigma} + h_{i,r,t,\sigma}\right]\end{aligned} \tag{6}$$

The lower-level constraints incorporate the AC-OPF model from Eq. (6) to (21), (23) and (24), applying to all $t \in \Omega_1$, $(i,j) \in \Omega_2 \vee i \in \Omega_3$, and $\forall\sigma \in \Omega_6$, where: l represents the annual load growth rate (in percentage); while voltages (V) and their phase angles (θ) must satisfy the long-term active and reactive power balance conditions, as defined in Eqs. (8) and (9).

$$S^2_{(i,j),t,\sigma} = P^2_{(i,j),t,\sigma} + Q^2_{(i,j),t,\sigma} \tag{7}$$

$$\sum_{(i,j)\in\Omega_2} P(V,\theta)_{(i,j),t,\sigma} + \cos(\theta)\cdot(D_{i,t} + d_{i,t,\sigma} - g_{i,t,\sigma}) = 0 \tag{8}$$

$$\sum_{(i,j)\in\Omega_2} Q(V,\theta)_{(i,j),t,\sigma} + \sin(\theta)\cdot(D_{i,t} + d_{i,t,\sigma} - g_{i,t,\sigma}) = 0 \tag{9}$$

$$P(V,\theta)_{(i,j),t,\sigma} = V_{i,t,\sigma} \cdot \sum_{(i,j)\in\Omega_2} V_{j,t,\sigma} \cdot \left[G_{(i,j),t} \cdot \cos\theta_{(i,j),t,\sigma} + B_{(i,j),t} \cdot \sin\theta_{(i,j),t,\sigma}\right] \tag{10}$$

$$Q(V,\theta)_{(i,j),t,\sigma} = V_{i,t} \cdot \sum_{(i,j)\in\Omega_2} V_{j,t,\sigma} \cdot \left[G_{(i,j),t} \cdot \sin\theta_{(i,j),t,\sigma} - B_{(i,j),t} \cdot \cos\theta_{(i,j),t,\sigma}\right] \tag{11}$$

$$|P_{(i,j),t,\sigma}| \leq \overline{P}_{(i,j),t} \tag{12}$$

$$|Q_{(i,j),t,\sigma}| \leq \overline{Q}_{(i,j),t} \tag{13}$$

$$\underline{V}_{i,t} \leq V_{i,t}, \sigma \leq \overline{V}_{i,t} \tag{14}$$

$$D_{(i,t+1)} = D_{(i,t)} \cdot (1+l)^t \tag{15}$$

The constructed and planned equipment are integrated into the availability matrix ($\mathcal{A}$) subjected to vectors modeling planned outages (ϖ) and failures (f) for each uncertain scenario (σ) in Ω_6 and stage (t) of the planning process in Ω_1. The equipment availability cause direct impact on $C^{o\&m}_{t,\sigma}$ and $C^{unr}_{t,\sigma}$.

$$\mathcal{A}_{(i,j),t,\sigma} = A \cdot (x + x_0) \cdot \varpi_{(i,j),t} \cdot f_{(i,j),t,\sigma} \tag{16}$$

$$0 \leq \varpi_{(i,j),t} \leq 1 \tag{17}$$

$$0 \leq f_{(i,j),t,\sigma} \leq 1 \tag{18}$$

Power systems should redirect flows during faults or outages with minimal service disruption, ensuring user demand under the N-1 reliability guideline. The planned solution (x) with the initial topology (x_0) must have redundancy for outages. The N-1 safety criterion matrix (A) in Eq. (16) adds reliability to the TEP task.

The transmitted apparent power from node S_i to node S_j is constrained by (19), considering the expected availability matrix $\mathcal{A}$ for both the initial system topology x_0 and the planned transmission assets x. The overload rate (Θ) defines the maximum overload allowed in the transmission network. The overload (φ) in branches (i,j) expressed in Eq. (20) is limited by 20% of its nominal power flow capability ($\overline{S}_{(i,j)}$).

$$\mathcal{A}_{(i,j),t,\sigma} \cdot S_{(i,j),\sigma} \leq \overline{S}_{(i,j)} \cdot \Theta \tag{19}$$

$$\varphi_{(i,j),\sigma} = S_{(i,j),\sigma} - \overline{S}_{(i,j)} \tag{20}$$

$$\varphi_{(i,j),\sigma} = \begin{cases} \varphi_{(i,j),\sigma}, & \text{if } \varphi_{(i,j),\sigma} > 0 \\ 0, & \text{if } \varphi_{(i,j),\sigma} \leq 0 \end{cases} \tag{21}$$

*3) **Unreliability costs**:* As shown in Equations (22), (23) and (24), $C^{unr}_{t,\sigma}$ depends on $EENS$ and short-term load shedding ($\mathcal{L}$), with d as short-term demand and D as long-term demand. The penalization factor γ is set at 10^{12} to prevent deterministic $EENS$, while the Value of Lost Load ($VoLL$) is 10 USD/kWh, accounting for demand uncertainties [20].

$$\min_{\{\mathcal{L}\}} C^{unr}_{t,\sigma} = \left[\sum_{i\in\Omega_3} \gamma \cdot EENS_{i,t} + VOLL \cdot \mathcal{L}_{i,t,\sigma}\right] \tag{22}$$

$$EENS_{i,t} = D_{i,t} + S_{(i,j),t} - g_{i,t,} \tag{23}$$

$$\mathcal{L}_{i,t,\sigma} = D_{i,t,\sigma} + d_{i,t,\sigma} + S_{(i,j),t,\sigma} - g_{i,t,\sigma} \tag{24}$$

C. Carbon Emissions

Burning fossil fuels for electricity and heat contributes significantly to global emissions. As in [23], [24], this work prioritizes green megawatts over non-renewable sources, aligning with global efforts to reduce GHG emissions. Thus, GHG emissions are included in the optimization process in Eq. (25), with emission rates per MWh (E) shown in Table III.

$$\min_g Z_2 = \rho \sum_{\sigma\in\Omega_6} \sum_{t\in\Omega_1} \sum_{i\in\Omega_3} g_{i,t,\sigma} \cdot E_i(CO_2, N_2O, SF_6) \tag{25}$$

D. Relative Flexibility Index (RFI)

The RFI is a quantitative measure used to assess the adaptability of a system, particularly in power grids and energy infrastructure. It evaluates how efficiently a system can respond to uncertainties, such as demand fluctuations, renewable energy variability, and unexpected failures. The RFI is typically computed by comparing the operational performance of a system under different scenarios, considering constraints such as network capacity, resource availability, and response time [25], [26]. A higher RFI indicates better resilience, while a lower RFI signals rigidity and vulnerabilities. In this work, RFI refers to grid flexibility as described in Eq. (26).

$$\max Z_3 = RFI = \frac{S_{flex}}{\overline{D}_{max}} \tag{26}$$

$$S_{flex} = min\left(\sum_{(i,j)\in\Omega_2} \overline{S}_{(i,j),t} - \sum_{(i,j)\in\Omega_2} S_{(i,j),t}\right) \tag{27}$$

$$\overline{D}_{max} = max \sum_{i\in\Omega_3} (D_{i,t} + d_{i,t,\sigma}) \tag{28}$$

III. Methodology

This study assesses ERCOT system resilience under stress and proposes a TEP that includes CC and EWEs to mitigate potential damages. It starts by constructing a set of stressed scenarios to model uncertainties accurately. In the second stage, a scenario reduction technique is applied to mitigate the computational burden. In the third stage, the optimization process is led by the NSGA-II algorithm in parallel to MATPOWER AC-OPF MIP solver aiming at evaluating the proposed TEP solutions [19].

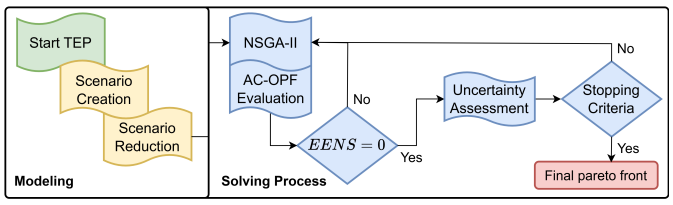

Fig. 1: Flowchart of the proposed methodology.

This study integrates a metaheuristic algorithm (NSGA-II), a computation-driven approach inspired by Genetic Algorithms (GA), with a self-adaptive mechanism to prevent premature convergence and mitigate potential discrepancies from gradient-based algorithms. Key input parameters include the

population size, the number of replications, and the maximum generations, serving as one of the stopping criteria. Further details on the NSGA-II algorithm are available in [27].

A. Scenario Creation

Following the methodology in [14], the ERCOT system was evaluated under stress by generating 300 challenging operating conditions. These scenarios incorporated both long-term uncertainties and short-term fluctuations, leveraging a Monte Carlo-based approach. Figure 2 presents the variations in PV generation over time, comparing scenarios that account for climate change (CC) and extreme weather events (EWEs) against those that do not. The influence of climate change on solar irradiation results in a projected increase in PV generation throughout the planning period.

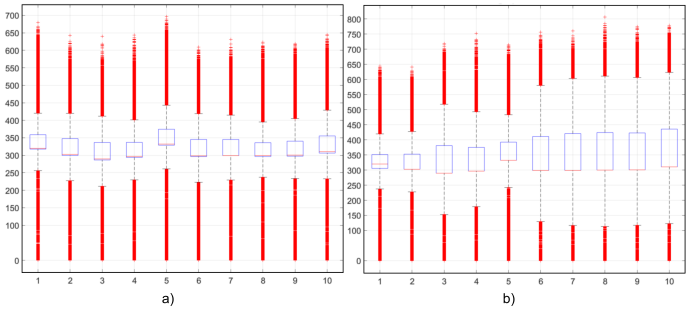

Fig. 2: Boxplot of PV generation (in MW on Y-axis) over each year of the planning Horizon (X-axis). **a)** shows the PV generation disregarding climate change, while **b)** consider CC and EWEs to compose the scenario set. [14]

B. Scenario reduction

Given the mathematical complexity of an NP-hard MINLP problem coupled with the scenario set, the planner must consider the computational time required for each iteration of the optimization process. Therefore, a scenario reduction technique was deployed to mitigate the computational burden while preserving solution accuracy by identifying critical operational scenarios across electrical zone-season pairings throughout the planning horizon: *i)* demand peak; *ii)* net-load peak; *iii)* maximum RESs generation regardless of demand; *iv)* maximum RESs feed-in during valley demand.

Pinpointing gross and net load peaks enables efficient resource allocation and capacity planning to meet demand requirements. Additionally, assessing the fluctuation of RESs contribution by identifying minimum and maximum feed-in during peak and valley demand periods captures key operational states pivotal to system performance and resilience.

IV. Simulations and Analysis

A. Outline of the tests

This section assesses the impact of HILP events, specifically CC and EWEs, on Transmission Expansion Planning. Two simulations were conducted on the ACTIVSg2000 test system to achieve this goal:

- **Simulation 1:** TEP task considering CC and EWEs.
- **Simulation 2:** Testing Pareto solutions under the extreme conditions that hit Texas in February 2021.

ACTIVSg2000 is a synthetic 2000-bus test case developed to represent the Texas bulk power system, as detailed in [17]. It includes transmission networks at 115, 161, 230 and 500 kV to better simulate the ERCOT grid.

B. Texas Rotating Outages

In February 2021, a severe snowstorm devastated Texas, freezing gas pipelines and turbine blades, drastically reducing the state's power generation capacity. The storm caused unprecedented generation losses, with 61.8 GW knocked offline [28]. During that event, demand spiked to nearly 70 GW, while 35 GW of coal, nuclear, and gas power plants went offline, disrupting the ERCOT system. Figure 3 depicts this terrifying scenario.

The financial impact was staggering, with losses from infrastructure damage and disrupted productivity estimated at $130 BUSD in Texas and $155 BUSD nationwide [4]–[6]. This decline in electricity generation persisted until February 19, resulting in $EENS = 998.8$ GWh. Unforeseeable events are an operational reality, but their consequences could have been mitigated with more resilient network planning and protective measures, transforming black swans into grey ones [13], [29].

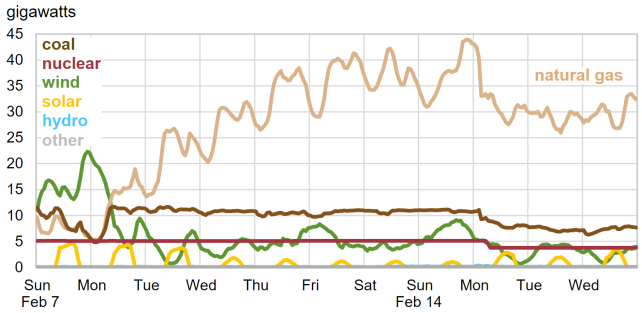

Fig. 3: ERCOT hourly net generation by energy source (Feb 7 – Feb 17, 2021) [30]

C. Form EIA-860

Form EIA-860 is a U.S. Energy Information Administration (EIA) survey that collects data on the status, characteristics, and operations of electric power plants with 1 MW or greater capacity [16]. It includes information on generator types, fuel sources, planned capacity additions, and environmental controls, supporting analysis of the nation's power generation infrastructure. Thus, Form EIA-860 is used in this paper as the generation expansion plan, allowing a better fit with the ERCOT plan. Figure 5 illustrates the coal-fired decommissioning plan, while Fig. 6 shows the planned RESs penetration.

D. Simulations

The simulation utilized scenarios covering long-term uncertainties like economic factors, demand growth, and CC, along

with short-term fluctuations such as real-time load variations, wind speeds, solar irradiation, and extreme weather events.

The simulation utilized scenarios covering both long-term uncertainties, such as economic factors, demand growth, and CC impacts, as well as short-term fluctuations, including real-time load variations, wind speeds, solar irradiation, and EWEs. For the NSGA-II algorithm governing upper-level decisions, the initial population consisted of 20 particles, with each iteration involving 3 replicated populations for analysis. As a stopping criterion, the simulation halted if 20 consecutive iterations showed no improvement in the Pareto front, with a maximum of 200 iterations. The planning horizon spanned 10 years in simulation 1, while in simulation 2, it represents 120 hours starting from Feb. 15 at 00:00.

1) ***Simulation 1*** *- TEP considering CC and EWEs:*
The simulation results indicate that each iteration took an average of 7 minutes and 30 seconds, with the algorithm reaching convergence after 38 iterations. A key insight from the analysis is the relationship between transmission investments, the Resilience Flexibility Index (RFI), and GHG emissions. As more capital is correctly allocated to transmission infrastructure, RFI tends to increase, allowing the system to better adapt to uncertainties and operational stress. Simultaneously, CO_2 emissions tend to decrease, suggesting that a more flexible grid facilitates the integration of RESs. However, the relationship between RFI and emissions is not strictly linear, indicating that other operational factors influence the trade-off.

From a decision-making perspective, risk-averse stakeholders might prioritize higher RFI, valuing system adaptability and robustness under extreme conditions. Conversely, risk-prone decision-makers may focus on minimizing costs, favoring solutions that require lower investments. To support decision-making, this study provides a multi-objective perspective, enabling planners to evaluate different expansion strategies and balance their preferences between system flexibility, environmental impact, and financial constraints. Figure 4 shows the non-dominant solutions.

2) ***Simulation 2*** *- Testing Pareto solutions under the extreme conditions that hit Texas in February 2021:*
After obtaining the Pareto front with the suggested TEP solutions in Simulation 1, this study evaluates their resilience under conditions similar to those in Texas in February 2021. To perform this test, a 120-hour generation contingency was simulated using the ACTIVSg2000 model [2], [3], [17], [30].

In this way, all the non-dominated solutions on the Pareto front surface were tested with the aim of achieving the one that behaves better under extreme conditions. The metric used to evaluate the TEP solutions was $EENS$.

E. Discussion

This HILP event emphasized the need for weather-resistant infrastructure and adaptable practices due to shifting climate patterns. Therefore, it was tested all solutions from Simulation 1 against the Texas crisis scenario to determine their Expected Value (EV) and Expected Energy Not Supplied ($EENS$)

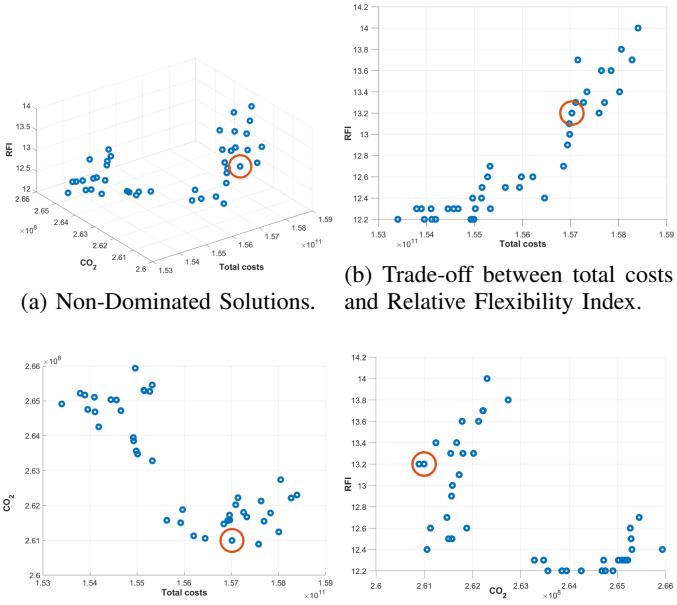

(a) Non-Dominated Solutions.

(b) Trade-off between total costs and Relative Flexibility Index.

(c) Trade-off between total costs and greenhouse emissions.

(d) Trade-off between RFI and greenhouse emissions.

Fig. 4: Non-Dominated Solutions from MO-TEP: Trade-Off Analysis Between Investment, GHG Emissions, and RFI. The red circle highlights the best solution in Simulation 2.

TABLE I: Selected Solution for Risk-Averse Decision-Makers.

Year	New connections	Year	New connections
1	1004-3133, 1037-1071	2	1048-1047, 1053 1081, 1079-1071
3	3048-1079, 2021 2002, 2113-8126	4	6264-6263, 8126-5049
5	6335-6043, 1079-1071	6	2101-5083, 4012-4103
7	7235-7315, 2127-5164	8	7043-7042
9	2017-2096, 2017-2127	10	2127-2011

during the event. Table II displays the economic difference between the proposed solutions and the current infrastructure.

TABLE II: MO-TEP Result by Planning Horizon.

Metric	Sim. 1 10 years	Sim. 2 120h of crisis	Estimated Damages in ERCOT (Feb. 2021)
C^{inv} [BUSD]	0.753	0.753	-
$C^{o\&m}$ [BUSD]	121.335	0.178	-
C^{unr} [BUSD]	0.001	119.75	-
EV [BUSD]	122.089	120.681	$130∼$155 [4]
$EENS$ [GWh]	-	812.45	998.8 [5]

V. Conclusion

Adopting an environmentally conscious approach requires a major transformation of power systems. As RESs integration grows, so does grid uncertainty. This study accounts for perturbations from CC and EWEs, strengthening TEP robustness. Although incorporating these uncertainties raises investment costs compared to traditional TEP methods, it makes networks more resilient to HILP events. However, implementing this

shift toward a more resilient ERCOT bulk system demands political commitment, significant financial investments, and a transition to a risk-averse approach.

REFERENCES

[1] Intergovernmental Panel on Climate Change (IPCC), *Climate Change 2023: Synthesis Report. Contribution of Working Groups I, II and III to the Sixth Assessment Report*, pp. 35–115. Switzerland: IPCC, 2023.

[2] M. O'Shea, R. Goel, and R. Miller, "Breaking down the texas winter blackouts: what went wrong?," Mar. 2021. Accessed: Jan. 20, 2025.

[3] J. W. Busby, K. Baker, M. D. Bazilian, A. Q. Gilbert, E. Grubert, V. Rai, J. D. Rhodes, S. Shidore, C. A. Smith, and M. E. Webber, "Cascading risks: Understanding the 2021 winter blackout in texas," *Energy Research & Social Science*, vol. 77, p. 102106, 2021.

[4] M. Puleo, "Damages from feb. winter storms could be as high as $155 billion," Mar. 2021. Accessed: Jan. 20, 2025.

[5] D. Wu, X. Zheng, A. Menati, L. Smith, B. Xia, Y. Xu, C. Singh, and L. Xie, "How much demand flexibility could have spared texas from the 2021 outage?," *Advances in Applied Energy*, vol. 7, p. 100106, 2022.

[6] A. Younesi, H. Shayeghi, Z. Wang, P. Siano, A. Mehrizi-Sani, and A. Safari, "Trends in modern power systems resilience: State-of-the-art review," *Renew. Sust. Energy Reviews*, vol. 162, p. 112397, 2022.

[7] Paris Agreement, "Paris climate agreement," in *report of the conf. of the parties to the United Nations framework convention on climate change (21st session, 2015: Paris). Retrived December*, vol. 4, 2015.

[8] R. He, L. Luo, A. Shamsuddin, and Q. Tang, "Corporate carbon accounting: A literature review of carbon accounting research from the kyoto protocol to the paris agreement," *Accounting & Finance*, vol. 62, no. 1, pp. 261–298, 2022.

[9] S. Bouckaert, A. F. Pales, C. McGlade, U. Remme, B. Wanner, L. Varro, D. D'Ambrosio, and T. Spencer, "Net zero by 2050: A roadmap for the global energy sector," 2021.

[10] European Commission, "European green deal: Eu agrees stronger legislation to accelerate the rollout of renewable energy," 2023.

[11] J. Qiu, H. Yang, Z. Y. Dong, J. Zhao, F. Luo, M. Lai, and K. P. Wong, "A probabilistic transmission planning framework for reducing network vulnerability to extreme events," *IEEE Transactions on Power Systems*, vol. 31, no. 5, pp. 3829–3839, 2016.

[12] L. E. Oliveira, J. T. Saraiva, J. A. D. Massignan, and P. V. Gomes, "Integration of business climate resilience on the transmission expansion planning over the low-carbon energy transition," in *2022 18th InternAtional Conf. on the European Energy Market (EEM)*, 2022.

[13] L. E. de Oliveira, P. Vilaça, J. T. Saraiva, and J. A. Massignan, "Cascade failures analyses improving resilience on transmission expansion planning," in *2023 IEEE Belgrade PowerTech*, pp. 01–06, IEEE, 2023.

[14] L. E. de Oliveira, J. T. Saraiva, and P. V. Gomes, "Risk adverse optimization on transmission expansion planning considering climate change and extreme weather events - the texas case," in *2024 20th International Conference on the European Energy Market (EEM)*, 2024.

[15] P. Vilaça, L. Oliveira, and J. Saraiva, "A congestion-based local search for transmission expansion planning problems," *Swarm and Evolutionary Computation*, vol. 83, p. 101422, 2023.

[16] U.S. Energy Information Administration (EIA), "Form eia-860 detailed data with previous form data (eia-860a/860b)." Electric power annual, 2023. Accessed: January 25, 2025.

[17] A. B. Birchfield, T. Xu, K. M. Gegner, K. S. Shetye, and T. J. Overbye, "Grid structural characteristics as validation criteria for synthetic networks," *IEEE Trans. on Power Systems*, vol. 32, pp. 3258–3265, 2017.

[18] W. Li, *Risk assessment of power systems: models, methods, and applications*. John Wiley & Sons, 2014.

[19] R. D. Zimmerman and C. E. Murillo-Sánchez, "Matpower," Oct. 2020.

[20] A. Khodaei and M. Shahidehpour, "Microgrid-based co-optimization of generation and transmission planning in power systems," *IEEE Transactions on Power Systems*, vol. 28, no. 2, pp. 1582–1590, 2013.

[21] P. Kayal and C. Chanda, "Optimal mix of solar and wind distributed generations considering performance improvement of electrical distribution network," *Renewable Energy*, vol. 75, pp. 173–186, 2015.

[22] A. R. Jordehi, "How to deal with uncertainties in electric power systems? a review," *Renewable and Sustainable Energy Reviews*, vol. 96, 2018.

[23] Y. Sun, C. Kang, Q. Xia, Q. Chen, N. Zhang, and Y. Cheng, "Analysis of transmission expansion planning considering consumption-based carbon emission accounting," *Applied energy*, vol. 193, pp. 232–242, 2017.

[24] V. Asgharian, *Alternative low-carbon generation and transmission expansion planning models for power systems with limited clean energy resources*. PhD thesis, University of British Columbia, 2021.

[25] H. Mazaheri, M. Moeini-Aghtaie, M. Fotuhi-Firuzabad, P. Dehghanian, and M. Khoshjahan, "A linearized transmission expansion planning model under n- 1 criterion for enhancing grid-scale system flexibility via compressed air energy storage integration," *IET Generation, Transmission & Distribution*, vol. 16, no. 2, pp. 208–218, 2022.

[26] R. Artis, M. Shivaie, and P. Weinsier, "A flexibility-based multi-objective model for contingency-constrained transmission expansion planning incorporating large-scale hydrogen/compressed-air energy storage systems and wind/solar farms," *Jour. of Energy Storage*, vol. 70, p. 108086, 2023.

[27] K. Deb, A. Pratap, S. Agarwal, and T. Meyarivan, "A fast and elitist multiobjective genetic algorithm: Nsga-ii," *IEEE Transactions on Evolutionary Computation*, vol. 6, no. 2, pp. 182–197, 2002.

[28] FERC and NERC, "February 2021 cold weather grid operations: Preliminary findings and recommendations," Feb. 2021.

[29] N. N. Taleb, *The black swan: The impact of the highly improbable*, vol. 2. Random house, 2007.

[30] EIA, "Extreme winter weather is disrupting energy supply and demand, particularly in texas," Feb 2021.

[31] U.S. Environmental Protection Agency (EPA), "Greenhouse gas equivalencies calculator - calculations and references," 2024.

[32] I. Peña, C. B. Martinez-Anido, and B.-M. Hodge, "An extended ieee 118-bus test system with high renewable penetration," *IEEE Transactions on Power Systems*, vol. 33, no. 1, pp. 281–289, 2018.

APPENDIX

TABLE III: Emission Rates per Energy Source [31], [32].

Energy Source	**CO_2 [kg/MWh]**	**N_2O [g/MWh]**	**SF_6 [mg/MWh]**
Biomass	130	0.177	5.79
Gas Combined-cycle turbines	500	0.079	0.60
Gas combustion turbines	500	0.079	0.60
Oil combustion turbines	850	0.177	5.79
Geothermal units	70	0.177	5.79
Hydro power plants	100	0.177	5.79
Internal Combustion Engines	550	0.079	0.60
Photovoltaic (solar)	40	0.177	5.79
Coal-Fired Steam Turbines	1050	0.382	330.30
Gas-Fired Steam Turbines	550	0.079	0.60
Wind power	10	0.357	5.79
Nuclear power plants	118	0.079	0.60

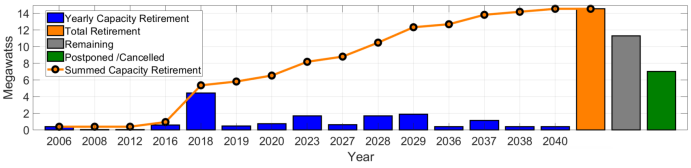

Fig. 5: Retirement plan for coal-fired Megawats in Texas (2006 – 2040). Data source: [16].

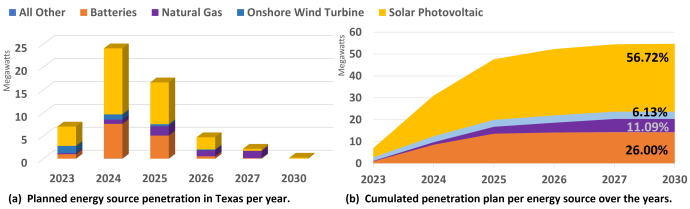

Fig. 6: Planned energy source penetration in Texas (2023 – 2030). Data source: [16].